



doi:10.1016/S0016-7037(03)00261-8

## Presolar spinel grains from the Murray and Murchison carbonaceous chondrites

ERNST ZINNER,<sup>1,\*</sup> SACHIKO AMARI,<sup>1</sup> ROBERT GUINNESS,<sup>1</sup> ANN NGUYEN,<sup>1</sup> FRANK J. STADERMANN,<sup>1</sup> ROBERT M. WALKER,<sup>1</sup> and ROY S. LEWIS<sup>2</sup><sup>1</sup>Laboratory for Space Sciences and the Physics Department, Washington University, St. Louis, MO 63130, USA<sup>2</sup>Enrico Fermi Institute, University of Chicago, 5630 Ellis Avenue, Chicago, IL 60637, USA

(Received December 23, 2002; revised 9 April 2003; accepted in revised form April 9, 2003)

**Abstract**—With a new type of ion microprobe, the NanoSIMS, we determined the oxygen isotopic compositions of small ( $<1\mu\text{m}$ ) oxide grains in chemical separates from two CM2 carbonaceous meteorites, Murray and Murchison. Among 628 grains from Murray separate CF (mean diameter  $0.15\mu\text{m}$ ) we discovered 15 presolar spinel and 3 presolar corundum grains, among 753 grains from Murray separate CG (mean diameter  $0.45\mu\text{m}$ ) 9 presolar spinel grains, and among 473 grains from Murchison separate KIE (mean diameter  $0.5\mu\text{m}$ ) 2 presolar spinel and 4 presolar corundum grains. The abundance of presolar spinel is highest (2.4%) in the smallest size fraction. The total abundance in the whole meteorite is at least 1 ppm, which makes spinel the third-most abundant presolar grain species after nanodiamonds (if indeed a significant fraction of them are presolar) and silicon carbide. The O-isotopic distribution of the spinel grains is very similar to that of presolar corundum, the only statistically significant difference being that there is a larger fraction of corundum grains with large  $^{17}\text{O}$  excesses ( $^{17}\text{O}/^{16}\text{O} > 1.5 \times 10^{-3}$ ), which indicates parent stars with masses between 1.8 and  $4.5 M_{\odot}$ . Copyright © 2003 Elsevier Ltd

### 1. INTRODUCTION

In 1987 Tang and Anders (Tang and Anders, 1988; Tang et al., 1988) prepared, by physical and chemical separation, a residue from the CM2 carbonaceous chondrite Murray. This residue, Murray CF (Fig. 1) contains high concentrations of the noble gas components Ne-E(H) and Xe-S (Tang and Anders, 1988). Subsequent analysis of CF by transmission electron microscopy, Raman laser microprobe spectroscopy and ion microprobe analysis led to the first identification of presolar silicon carbide (Bernatowicz et al., 1987; Zinner et al., 1987).

However, SiC constitutes  $< 10\%$  of Murray CF and most of the residue consists of spinel grains. Zinner and Tang (1988) measured O isotopic ratios in the CF residue with the Cameca IMS 3f ion microprobe at Washington University. Oxygen isotopic measurements require high mass resolution that allows the separation of the  $^{16}\text{OH}^-$  ion signal from that of  $^{17}\text{O}^-$ . In the IMS 3f ion probe, this leads to a large reduction in secondary ion transmission. Because of the small grain size of CF (average grain diameter of  $0.15\mu\text{m}$ ), measurements could not be made on single grains but were made on aggregates of thousands of grains. The results are shown in Figure 2. All CF analyses show excesses in  $^{17}\text{O}$  relative to the isotopic compositions of spinel grains in the Murchison carbonaceous chondrite (Clayton and Mayeda, 1984). Although this result hinted at the presence of presolar spinel grains, such a presence could not be clearly established and it took several years before the existence of presolar oxide grains in primitive meteorites was unambiguously demonstrated (Hutcheon et al., 1994; Nittler et al., 1994).

Most presolar oxide grains have large  $^{17}\text{O}$  excesses (Nittler et al., 1997) and if the O isotopic compositions of

the putative presolar grains in CF were the same as those of larger oxide grains we estimate that  $\sim 2\%$  of the CF spinel grains should be of presolar origin. The arrival of a new type of ion microprobe, the Cameca NanoSIMS (Stadermann et al., 1999a, 1999b, 2000), in our laboratory has opened the possibility of measuring the O isotopic composition of individual grains as small as those in Murray CF. The NanoSIMS has several novel features that make it the instrument of choice for the isotopic analysis of very small grains. First, at a mass resolving power of  $\sim 5000$ , necessary for O isotopic analysis, the secondary ion transmission is  $> 30$  times higher than that of the Cameca IMS 3f. Second, the NanoSIMS has miniaturized electron multipliers (Slodzian et al., 2003), four of which can be moved along the focal plane of the secondary ions. This means that O isotopic ratios can be measured simultaneously (“multidetector”). This not only increases the overall sensitivity for such measurements, but any change in the secondary ion signal, which, because of the small size of the grains, is unavoidable, does not affect the measured isotopic ratios as it would if magnetic peak jumping and just one detector were employed. Third, the NanoSIMS features a very small primary beam size. For  $\text{Cs}^+$  primary ions, beam diameters  $< 50\text{ nm}$  have been achieved and a beam diameter of  $100\text{ nm}$  is routine. The reason for this is that the primary ions are incident normal to the sample surface, along the same axis secondary ions are extracted. As a consequence, the immersion lens can be placed very close to the sample surface, resulting in a large demagnification of the primary beam diameter.

We took advantage of these new instrumental capabilities to measure O isotopic ratios of individual grains from Murray CF (average grain diameter  $0.15\mu\text{m}$ ). In addition, we measured the O isotopic ratios of grains from separates Murray CG (average grain size  $0.45\mu\text{m}$ ) and Murchison KIE (average grains size  $0.5\mu\text{m}$ ) (Fig. 1).

\* Author to whom correspondence should be addressed (ekz@wuphys.wustl.edu).

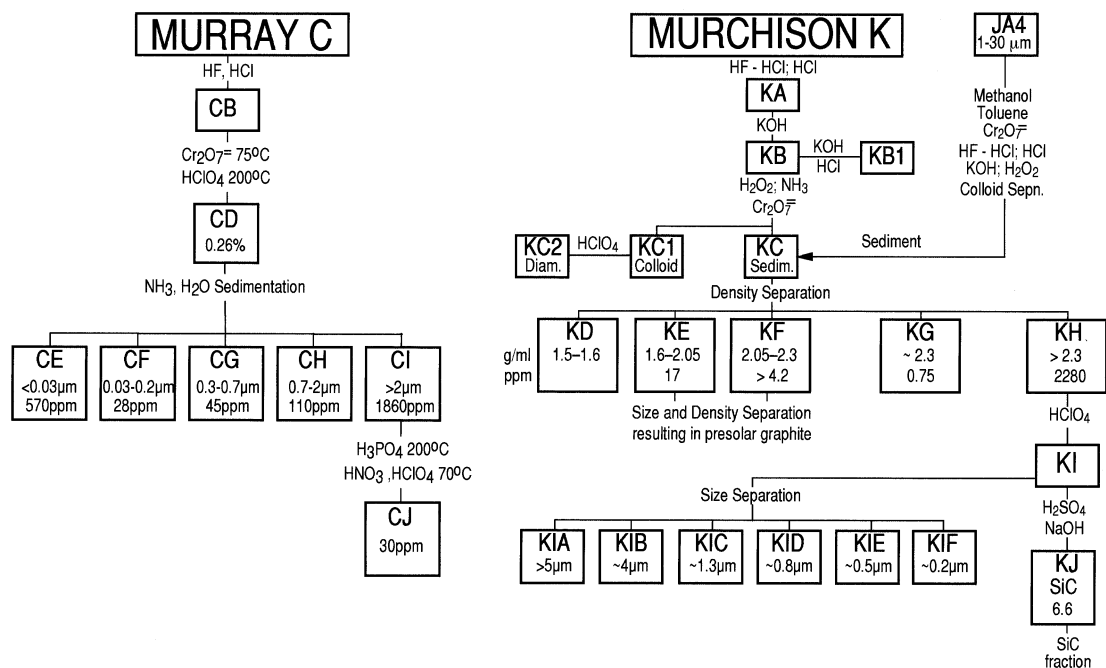


Fig. 1. Flowcharts for the separation of Murray residues CF and CG (Tang and Anders, 1988) and Murchison residue KIE (after Amari et al., 1994).

## 2. EXPERIMENTAL

Tang and Anders (1988) have described the separation of the Murray residues and Amari et al. (1994) that of the Murchison K series. Most of residue KI was further processed by dissolving spinel grains to obtain a separate consisting mostly of SiC. However, a fraction of KI was not treated in this way and was separated into different size

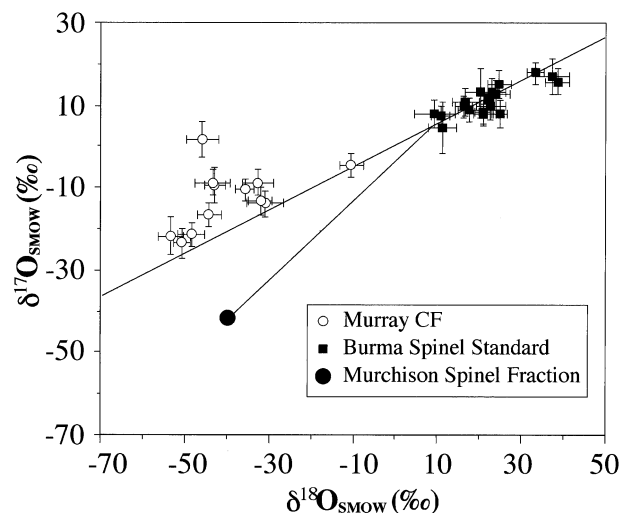


Fig. 2. Oxygen isotopic ratios measured in aggregates of spinel grains from Murray separate CF together with ratios measured in the Burma spinel standard. Data are from Zinner and Tang (1988). Also plotted are the ratios for the Murchison spinel fraction measured by Clayton and Mayeda (1984). The ratios are expressed as  $\delta$ -values, deviations from the SMOW standard ratios in per mil (‰). The two lines are the terrestrial mass fractionation line (slope 0.5) and the refractory inclusion line (slope 1).

fractions (Fig. 1). For NanoSIMS analysis, grains from the three selected separates were deposited from liquid suspension onto high purity gold foils, which had been pressed into a metal mount (an Al SEM stub in case of CF, a brass disk in case of the other two residues). Along with the meteoritic grains we deposited 1- $\mu\text{m}$   $\text{Al}_2\text{O}_3$  grains (polishing powder) and Murchison matrix in separate locations on the Au foils.

Oxygen isotopic measurements were made with the Cameca NanoSIMS ion microprobe. Three electron multipliers were used to count the negative secondary ions of the three O isotopes produced by bombardment with a 16-keV  $\text{Cs}^+$  beam of a few picoamperes in intensity. In addition, we detected the  $^{24}\text{MgO}^-$  signal at mass 40 to identify spinel grains. For part of the CF measurements we also detected the  $\text{AlO}^-$  signal at mass 43. In the NanoSIMS three different values for the exit slits are available to achieve different magnitudes of mass resolving power. For the measurement of  $^{16}\text{O}$ ,  $^{18}\text{O}$ , and  $\text{MgO}$  we used exit slits of 50  $\mu\text{m}$  width, which produce a mass resolving power  $M/\Delta M$  of  $\sim 3000$ , and for  $^{17}\text{O}$  an exit slit of 25  $\mu\text{m}$ , which produced a mass resolving power  $> 5000$  (the exact value depends on other tuning conditions), sufficient to exclude contributions from  $^{16}\text{OH}$ . During multidetection analysis, the magnetic field of the mass spectrometer was kept constant under NMR (nuclear magnetic resonance) control. In this way field values were kept within the limits required by the measurements for several hours.

Because individual electron multipliers do not have identical detection efficiencies, multidetection analysis requires calibration against a standard. We used terrestrial Al oxide grains as standards. The Murchison matrix sample was used to center on the  $\text{MgO}$  peak. Under our measurement conditions the  $^{28}\text{SiC}$  peak was not resolved from the  $\text{MgO}$  peak. Grains to be analyzed were identified from  $20 \times 20 \mu\text{m}^2$  raster images ( $256 \times 256$  pixels) of  $^{16}\text{O}^-$  ions and of secondary electrons (Fig. 3). Secondary electrons are created and extracted together with negative secondary ions and can be detected with a special detector. To obtain an analysis of a chosen grain, the primary ion beam was deflected onto the grain and rastered over a  $0.8 \times 0.8 \mu\text{m}^2$  area and the O isotope and  $\text{MgO}$  signals were counted in multidetection. A typical single grain analysis took only 1 min. The density of the meteoritic grains deposited on the mount was such that typically 20 to 40 grains were contained in the  $20 \times 20 \mu\text{m}^2$  area. Figure 3d shows a

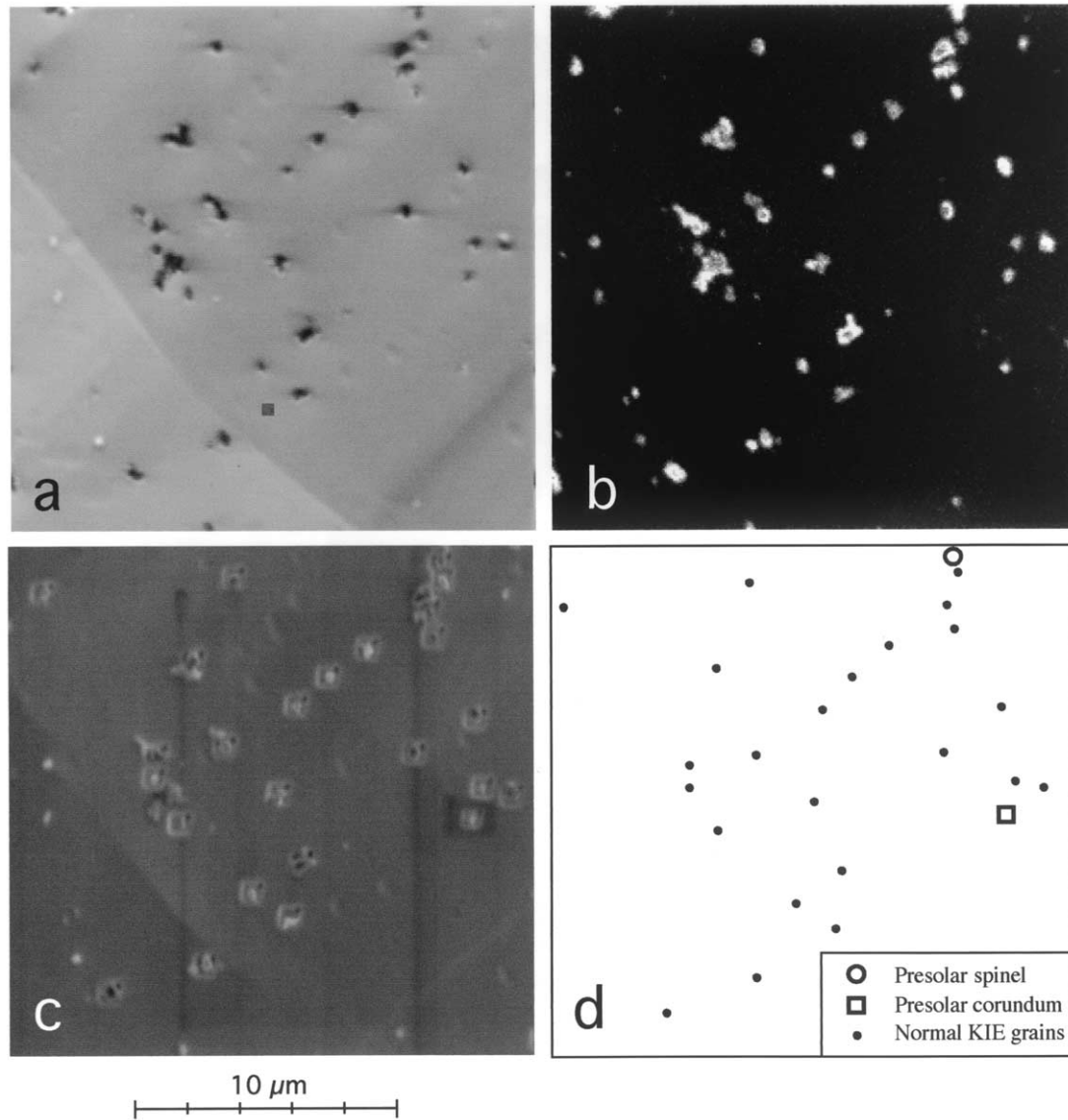


Fig. 3. Images of Murchison KIE grains that were deposited on gold and analyzed for their O isotopic compositions in the NanoSIMS. (a) Secondary electron image in the NanoSIMS. (b)  $O^-$  image. (c) SEM image obtained after NanoSIMS analysis showing the sputter squares produced by rastering the  $Cs^+$  primary ion beam around selected grains. (d) Coordinates of the analyzed grains. Two of them, one spinel and one corundum, are identified as presolar by their highly anomalous O isotopic compositions. One image is  $20\ \mu m$  on a side.

plot of the coordinates of the 25 grains that were analyzed in this area. Also shown is an SEM image of the area after analysis in which the little raster squares around analyzed grains can be seen (Fig. 3c). Two grains in this area turned out to be clearly presolar, one being a spinel, the other being a corundum grain. Before the beginning of isotopic analysis all measured peaks were centered into the exit slits of the different detectors by placing the detectors in the right positions along the focal plane and by using electrostatic deflection plates in front of each electron multiplier. Because of the small sizes of most meteoritic grains, this peak centering was done only on the standard and Murchison matrix grains. Although the various high voltages on lenses and deflectors as well as the magnetic field of the mass spectrometer are generally stable for many hours, we repeated peak centering during isotopic measurements on the standards, which were interspersed with measurements of the meteoritic grains.

For data analysis we corrected the ratios measured in the meteoritic grains by assuming that the standard grains have the SMOW (standard

mean ocean water) ratios of  $^{17}O/^{16}O = 0.0003829$  and  $^{18}O/^{16}O = 0.0020052$ . The  $^{18}O/^{16}O$  ratio is taken from Baertschi (1976), the  $^{17}O/^{16}O$  ratio is the average of many years of ion microprobe O isotopic measurements on various standards in our laboratory under the assumption of an exponential mass fractionation law during SIMS analysis. Although we actually do not know the exact isotopic composition of the  $Al_2O_3$  standard, for the identification of presolar grains we do not need to know it to any great accuracy because we identify presolar grains by their deviations from the bulk of meteoritic grains, most of which are undoubtedly of solar system origin. Furthermore, the standard grains are apparently not very far from SMOW in their ratios because the average compositions of the meteoritic spinel grains of apparent solar system origin are  $\delta^{17}O/^{16}O = -25\%$  and  $\delta^{18}O/^{16}O = -51\%$  for CF,  $\delta^{17}O/^{16}O = -52\%$  and  $\delta^{18}O/^{16}O = -55\%$  for CG, and  $\delta^{17}O/^{16}O = -51\%$  and  $\delta^{18}O/^{16}O = -43\%$  for KIE. These compositions are very similar to what has been found for spinel grains in carbonaceous meteorites (see also Fig. 2) and it should be noted that the

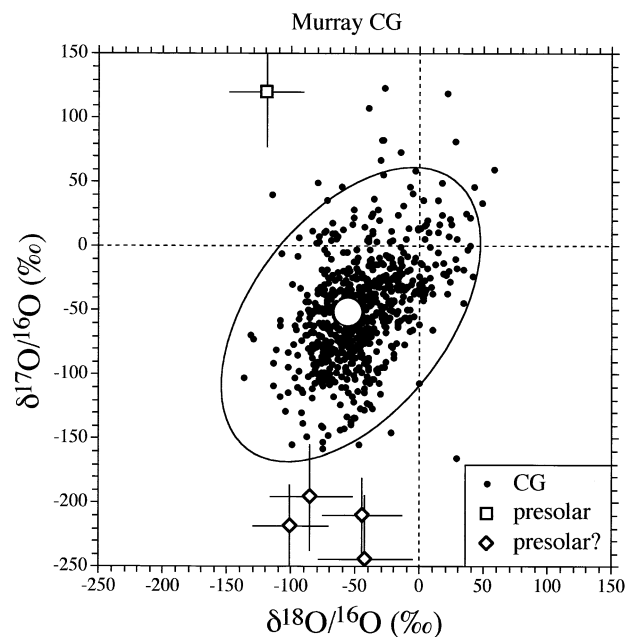


Fig. 4. This oxygen 3-isotope plot demonstrates our criteria for the identification of presolar grains. Shown are O isotopic ratios of CG grains having measurement errors  $< 10\%$ . No error bars are shown to avoid clutter. The small open symbols are for grains that are candidates to be of presolar origin. The large open circle is the average of all the "normal" grains. The ellipse around this average composition has axes that are three times the standard deviation in the direction of the correlation line for the CG grains and normal to it. A presolar grain is required to have a composition that is  $2\sigma$  away from this ellipse. The grain with the square symbol satisfies this requirement, the grains with the diamonds do not. Shown error bars are  $1\sigma$ .

differences between the averages of different separates are much smaller than the typical measurement errors on meteoritic grains during our measurements. For the measurement errors we combined the analytical errors (essentially errors due to counting statistics) with the standard deviations of measured ratios on individual standard grains from their average. These standard deviations ranged from 26 to 34‰ for the  $^{17}\text{O}/^{16}\text{O}$  ratio and from 32 to 49‰ for the  $^{18}\text{O}/^{16}\text{O}$  ratio for the measurements of the standards analyzed along with the three meteoritic grain separates.

There is no absolute criterion for identifying presolar grains by their anomalous isotopic ratios. For this study we considered them as presolar if their isotopic ratios plot clearly outside of the region occupied by the large majority of all meteoritic grains that had sufficiently small measurement errors. In quantitative terms we required that the isotopic compositions of presolar grains differ by  $> 3\sigma$  from the average compositions of all "normal" grains. In addition, we required that the presolar grains are  $> 2\sigma$  away from the  $3\sigma$  (standard deviation) ellipse of the distribution of the "normal" grains. This is demonstrated for the CG grains in Figure 4 in a 3-isotope- $\delta$ -value plot. The ellipse is aligned with the correlation line of all "normal" CG grains that have analytical errors of  $< 100\%$ . Its axes are three times the standard deviations from the average composition of the "normal" grains in the directions of the correlation line and normal to it. The reduced  $\chi^2$  of the variations of the compositions of the "normal" grains in these two directions is 0.94 and 0.83, respectively. The CG grains outside the  $3\sigma$  ellipse that are plotted as solid circles have large errors. The grain in the upper left of the plot is  $> 2\sigma$  away from the ellipse and we therefore classify it as a presolar grain. The four grains with low  $^{17}\text{O}/^{16}\text{O}$  ratios are closer than  $2\sigma$  to the ellipse and are therefore rejected. It is clear that this criterion is quite conservative and truly presolar grains might be rejected but we feel it to be better to err on the safe side.

### 3. RESULTS

The O isotopic ratios of the measured grains are shown in Figure 5, the ratios of grains we consider presolar are given in Table 1. As can be seen from the isotopic ratio plots in Figure 5, the isotopic compositions of grains we classified as presolar are clearly outside those of the vast majority of grains. As will be shown later, they are similar to those of grains previously considered to be presolar oxide grains (Nittler et al., 1997; Choi et al., 1998, 1999).

We have used the ion signal at mass 40 ( $\text{MgO}^-$  or  $\text{SiC}^-$ ) obtained from all the analyzed grains to obtain information about their mineralogy. From the separation of the residues as well as from previous studies of the composition of such residues (e.g., Tang and Anders, 1988; Tang et al., 1988; Amari et al., 1994) it is clear that they should be mainly composed of Al-Mg spinel ( $\text{MgAl}_2\text{O}_4$ ), SiC, and other refractory oxide phases such as corundum ( $\text{Al}_2\text{O}_3$ ) and hibonite ( $\text{CaAl}_{12}\text{O}_{19}$ ) that survived the chemical processing. Figure 6 shows the  $(\text{mass-40})^-/\text{O}^-$  or  $(\text{MgO}^- \text{ and/or } \text{SiC}^-)/\text{O}^-$  ratios of the analyzed grains plotted against the  $^{16}\text{O}^-$  count rate. As can be seen, most clearly for Murray CG and Murchison KIE, there is a fairly narrow range of  $(\text{mass-40})^-/\text{O}^-$  ratios  $\sim 4$  to  $6 \times 10^{-3}$  where most of the grains plot. This is the ratio we also observed in terrestrial spinel samples; thus the meteoritic grains plotting in this range are apparently spinel grains and the ion signal at mass 40 is  $\text{MgO}^-$ . This band is wider for the CF grains and seems to slope to smaller  $(\text{mass-40})^-/\text{O}^-$  ratios for low  $^{16}\text{O}^-$  count rates. The first fact probably has to do with contamination of grains and sample mount playing a larger role for small grains. The second fact most likely is a consequence of preferential sputtering effects. In larger grains we observed that at the beginning of a measurement the  $\text{O}^-$  signal rises much faster than the molecular ion signals such as  $\text{MgO}^-$  and  $\text{AlO}^-$ . For the smallest grains it is therefore not surprising that the  $\text{MgO}^-/\text{O}^-$  ratios are smaller than those measured in larger grains.

Besides spinel, the residues also contain grains with higher and lower  $(\text{mass-40})^-/\text{O}^-$  ratios. Such grains are relatively few in Murray CF and CG but represent major populations in Murchison KIE (Fig. 6). We actually had expected to find grains with higher  $(\text{mass-40})^-/\text{O}^-$  ratios. These must be SiC grains for which the ion signal at mass 40 is  $\text{SiC}^-$ , which under our measurement conditions was not separated from the  $\text{MgO}^-$  signal. Apparently, SiC grains in the residues developed a Si oxide rim during the chemical processing and could not be distinguished from oxide grains in the  $^{16}\text{O}^-$  images that were used to select grains for analysis. Indeed, as can be seen in Figure 6, grains with higher  $(\text{mass-40})^-/\text{O}^-$  ratios tend to have lower  $\text{O}^-$  count rates, especially grains from the residues CF and CG. To identify the mineralogy of grains in Murchison KIE, we obtained EDS (energy dispersive X-ray spectroscopy) spectra in the SEM. Grains with higher  $(\text{mass-40})^-/\text{O}^-$  ratios were confirmed to be SiC and grains in the narrow range of  $(\text{mass-40})^-/\text{O}^-$  ratios were found to be Al-Mg spinel. However, we found that most grains with lower ratios are Si oxide and only a small fraction of them ( $\sim 8\%$ ) are corundum grains. This was unexpected because the extensive treatment with HF that led to the separation of KIE (see Fig. 1) should have destroyed all silicates and essentially no Si oxide grains were identified in the Murray residues. Such grains in Murchison KIE are appar-

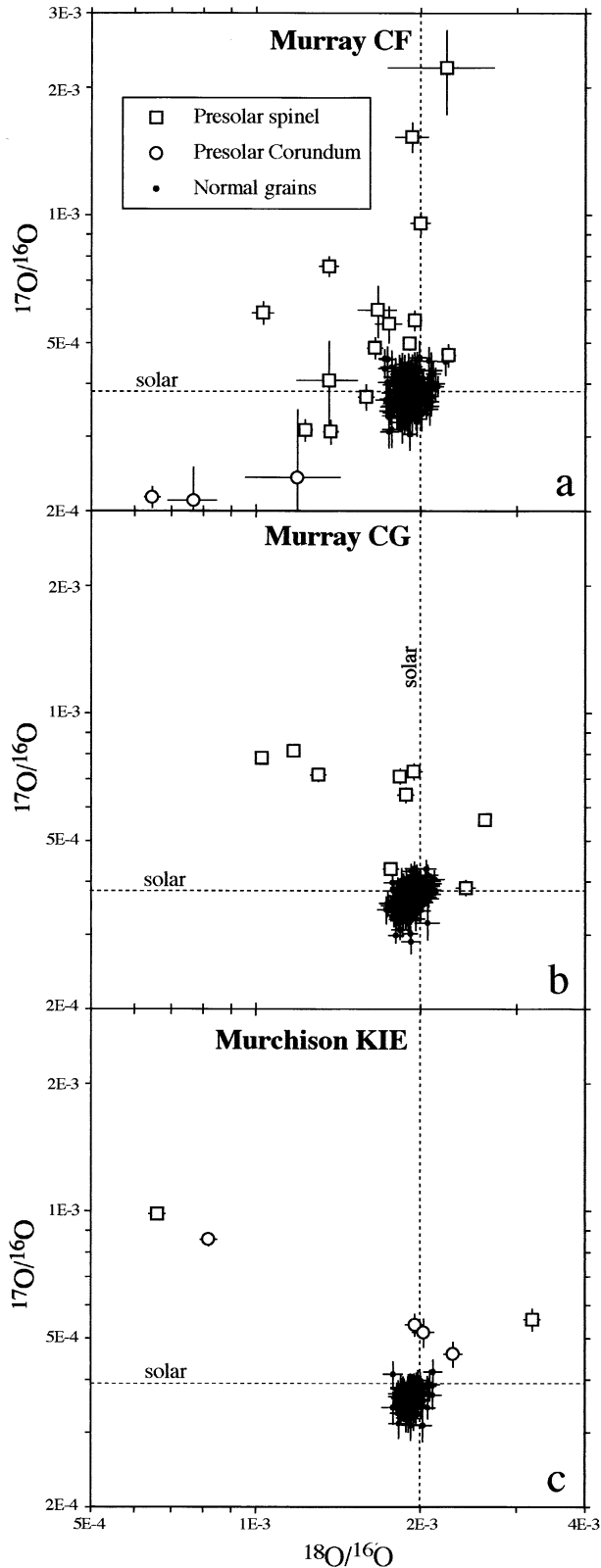


Fig. 5. Oxygen isotopic ratios of presolar spinel and corundum grains from the residues CF, CG, and KIE as well as those of “normal” grains. The broken lines indicate the solar (terrestrial) ratios of 0.000383 for  $^{17}\text{O}/^{16}\text{O}$  and 0.002005 for  $^{18}\text{O}/^{16}\text{O}$ .

Table 1. Oxygen isotopic ratios of presolar grains from Murray and Murchison separates.

	$^{17}\text{O}/^{16}\text{O} \pm 1\sigma$	$^{18}\text{O}/^{16}\text{O} \pm 1\sigma$
CF		
Spinel	0.002230 $\pm$ 0.000499	0.00223 $\pm$ 0.00049
	0.000498 $\pm$ 0.000018	0.00191 $\pm$ 0.00004
	0.000757 $\pm$ 0.000041	0.00136 $\pm$ 0.00006
	0.000372 $\pm$ 0.000026	0.00159 $\pm$ 0.00005
	0.000958 $\pm$ 0.000056	0.00200 $\pm$ 0.00008
	0.000588 $\pm$ 0.000035	0.00103 $\pm$ 0.00005
	0.000564 $\pm$ 0.000030	0.00195 $\pm$ 0.00006
	0.000467 $\pm$ 0.000028	0.00225 $\pm$ 0.00006
	0.001530 $\pm$ 0.000121	0.00193 $\pm$ 0.00013
	0.000486 $\pm$ 0.000028	0.00165 $\pm$ 0.00005
	0.000597 $\pm$ 0.000082	0.00167 $\pm$ 0.00014
	0.000308 $\pm$ 0.000020	0.00137 $\pm$ 0.00004
	0.000554 $\pm$ 0.000055	0.00175 $\pm$ 0.00010
	0.000311 $\pm$ 0.000018	0.00123 $\pm$ 0.00004
	0.000407 $\pm$ 0.000096	0.00136 $\pm$ 0.00017
Corundum	0.000212 $\pm$ 0.000042	0.00077 $\pm$ 0.00008
	0.000240 $\pm$ 0.000107	0.00119 $\pm$ 0.00024
	0.000216 $\pm$ 0.000012	0.00065 $\pm$ 0.00002
CG		
Spinel	0.000814 $\pm$ 0.000026	0.00117 $\pm$ 0.00003
	0.000782 $\pm$ 0.000023	0.00103 $\pm$ 0.00002
	0.000728 $\pm$ 0.000032	0.00194 $\pm$ 0.00007
	0.000715 $\pm$ 0.000026	0.00130 $\pm$ 0.00005
	0.000709 $\pm$ 0.000030	0.00183 $\pm$ 0.00005
	0.000560 $\pm$ 0.000018	0.00262 $\pm$ 0.00005
	0.000429 $\pm$ 0.000015	0.00177 $\pm$ 0.00006
	0.000387 $\pm$ 0.000016	0.00242 $\pm$ 0.00010
	0.000641 $\pm$ 0.000026	0.00188 $\pm$ 0.00007
KIE		
Spinel	0.000985 $\pm$ 0.000032	0.00066 $\pm$ 0.00002
	0.000555 $\pm$ 0.000034	0.00320 $\pm$ 0.00011
Corundum	0.000460 $\pm$ 0.000031	0.00230 $\pm$ 0.00009
	0.000517 $\pm$ 0.000040	0.00203 $\pm$ 0.00009
	0.000539 $\pm$ 0.000032	0.00195 $\pm$ 0.00007
	0.000857 $\pm$ 0.000031	0.00082 $\pm$ 0.00003

ently quartz grains that were introduced as contamination after HF treatment. A possibility is that they are SiC grains that were completely oxidized by the chemical processing (following HF treatment) but we could not detect any difference in size between the Si oxide and SiC grains. We might measure the Si isotopic compositions of the Si oxide grains but their provenance is of no concern for the present study.

Because four of the six KIE grains with large anomalies in oxygen have lower (mass-40) $^{-1}\text{O}^{-}$  ratios than spinel grains, it was important to establish the mineralogy of those grains. However, only grain A from KIE (see Fig. 6c) had enough material left that we could obtain a diagnostic EDS spectrum; this grain was thereby identified as corundum. In contrast, grain B that lies in the spinel band (Fig. 6c) gave an EDS spectrum characteristic of spinel. Since there was some material left of the other grains and SIMS is much more sensitive than EDS analysis, we went back to the NanoSIMS and measured the  $^{12}\text{C}^{-}$ ,  $^{13}\text{C}^{-}$ ,  $^{16}\text{O}^{-}$ ,  $^{28}\text{Si}^{-}$ , and  $\text{Al}^{16}\text{O}^{-}$  signals of the six presolar oxide grains as well as of other grains previously analyzed for their O isotopic ratios. All four presolar grains with (mass-40) $^{-1}\text{O}^{-}$  ratios lower than those of spinel grains yielded  $\text{AlO}^{-}/\text{O}^{-}$  ratios much higher than any of the quartz grains and are probably corundum (as mentioned above, one of them has an EDS spectrum characteristic of corundum) although we

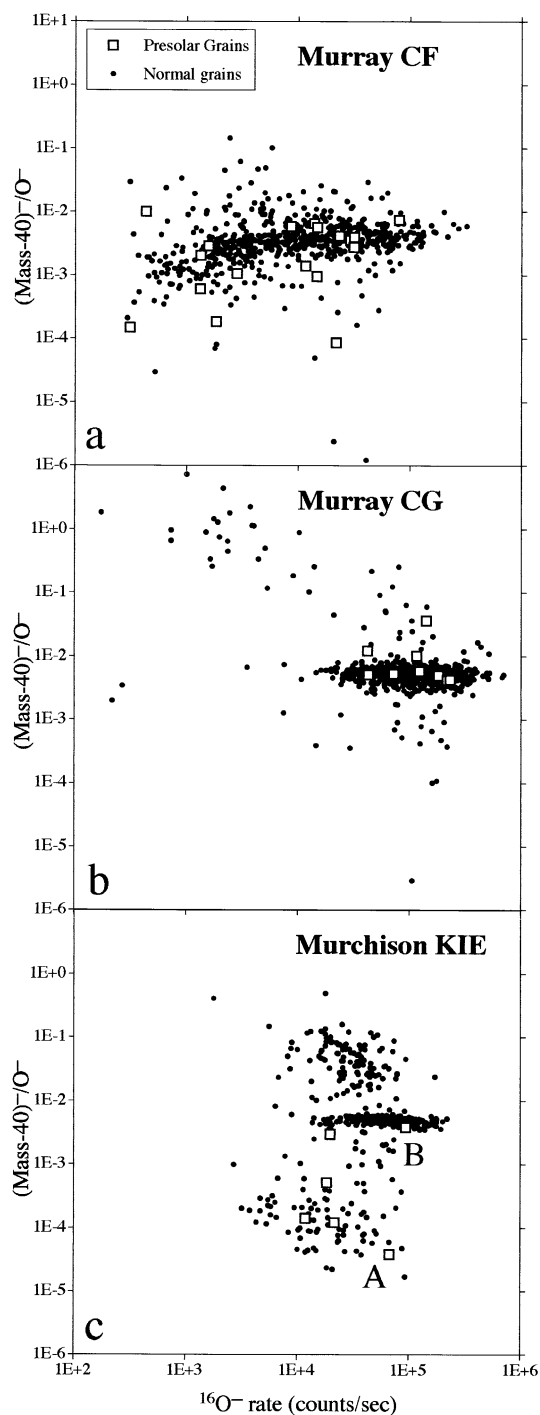


Fig. 6. Ion ratios of the signal at mass 40 relative to  $^{16}\text{O}^-$  of CF, CG and KIE grains are plotted against the  $^{16}\text{O}^-$  count rates during ion microprobe analysis. The mass 40 signal was used to monitor  $\text{MgO}^-$  from spinel grains but could not be separated from the  $\text{SiC}^-$  signal. In this plot spinel grains fall into a band with  $(\text{mass-40})^-/\text{O}^-$  ratios of  $\sim 4$  to  $6 \times 10^{-3}$ . Some presolar oxide grains plot below this band and are probably corundum, but hibonite cannot be excluded. Silicon carbide grains, whose surface was oxidized by laboratory chemical processing, give higher  $(\text{mass-40})^-/\text{O}^-$  ratios (actually  $\text{SiC}^-/\text{O}^-$  ratios). Most grains with lower apparent  $(\text{mass-40})^-/\text{O}^-$  ratios are quartz grains that must have been introduced by contamination. Grains A and B from residue KIE were identified as corundum and spinel, respectively, by EDS analysis in the SEM after isotopic analysis with the NanoSIMS.

cannot exclude hibonite. We note that, at least for  $> 1\text{-}\mu\text{m}$  grains, presolar hibonite is much less abundant than presolar corundum (Choi et al., 1999; Krestina et al., 2002).  $\text{MgO}^-/\text{O}^-$  ratios measured in the corundum standard grains are generally below  $2 \times 10^{-5}$ , but meteoritic corundum grains are not that pure and have a large range of Mg/Al ratios (Nittler, 1996; Choi et al., 1998). Grains with higher  $(\text{mass-40})^-/\text{O}^-$  ratios were all found to be presolar SiC grains with anomalous C isotopic ratios.

We thus tentatively classify the three presolar CF grains and four KIE grains with the lowest  $(\text{mass-40})^-/\text{O}^-$  ratios as corundum. One CF and one CG grain with ratios above the spinel band possibly had SiC stuck to them and, in principle, we cannot even exclude that they are corundum. We conclude (with some uncertainty) to have found 15 presolar spinel grains in Murray CF, 9 in Murray CG and 2 in Murchison KIE.

Unfortunately, the CF grains are so small that many of them are consumed during O isotopic analysis. However, this is not the case for the larger grains and in future studies we plan to obtain positive secondary ion images of Mg, Al, Si and Ca of the grains analyzed for their O isotopic ratios to help with the determination of their mineralogy (spinel, corundum, hibonite, SiC and contaminants). If we measure Ca (for the identification of hibonite) as  $\text{Ca}^{2+}$  we can measure all four elements in multidetection and even include  $^{26}\text{Mg}$  to look for evidence of  $^{26}\text{Al}$ .

#### 4. DISCUSSION

When we started this study, 183 presolar corundum grains but only 7 presolar spinel grains had been identified (Nittler et al., 1997; Choi et al., 1998; Nittler, unpublished results), giving the impression that presolar spinel is extremely rare (during the course of this study we have been made aware of 4 more presolar spinel grains). However, all previous studies have been made on grains  $> 1\text{ }\mu\text{m}$ . By analyzing  $< 1\text{-}\mu\text{m}$  grains in the NanoSIMS we have identified 26 presolar spinel grains and an additional 7 presolar corundum grains. The O isotopic compositions of our 26 spinel grains are plotted in Figure 7 together with those of 10 spinel grains found in other studies (Nittler et al., 1997; Choi et al., 1998; Nittler, unpublished results).

From the number of presolar oxide grains identified in this study we can make some estimates about their abundances. Table 2 gives the abundances of presolar oxide grains as fractions of the analyzed grains in the different residues and as fractions of the total meteorite. In column 4 we list the abundance of presolar spinel among all spinel grains of a given residue. We cannot do that (yet) for corundum because the abundance of corundum in the different residues is not well known. From EDS analysis,  $\sim 2\%$  of all grains in KIE appear to be corundum, which would mean that as many as half of corundum grains are presolar. Even within the limits imposed by the statistics of small numbers, it is clear that the relative abundance of presolar grains is highest among the smallest size fractions. Since we know the weight fractions of the two Murray separates (28 ppm for CF and 45 ppm for CG) relative to the whole meteorite (Tang and Anders, 1988; see Fig. 1), we can estimate the abundances of presolar spinel and corundum in this meteorite. They are given in columns 5 and 6 of Table 2. The abundance of presolar spinel in Murray thus appears to be

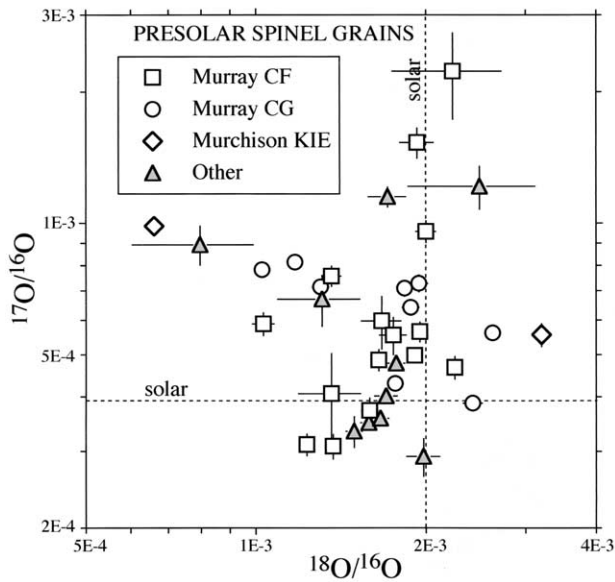


Fig. 7. Oxygen isotopic ratios of presolar spinel grains identified in this study as well as spinel grains identified by others (Nittler et al., 1997; Choi et al., 1998; Nittler, unpublished). One previously identified spinel grain is not shown in this figure; it lies off-scale at  $^{17}\text{O}/^{16}\text{O} = 1.25 \times 10^{-3}$  and  $^{18}\text{O}/^{16}\text{O} = 6.9 \times 10^{-3}$  (see Figs. 9 and 11). In this figure and in Figures 9 to 11 we have plotted  $^{17}\text{O}/^{16}\text{O}$  versus  $^{18}\text{O}/^{16}\text{O}$  ratios. This is in contrast to the convention of astronomers, who use  $^{16}\text{O}/^{17}\text{O}$  and  $^{16}\text{O}/^{18}\text{O}$  but in agreement with the convention of geo- and cosmochemists, who plot O isotopic ratios as  $\delta^{17}\text{O}/^{16}\text{O}$  and  $\delta^{18}\text{O}/^{16}\text{O}$  (usually shortened to  $\delta^{17}\text{O}$  and  $\delta^{18}\text{O}$ ) values (see Figs. 2 and 4). Oxygen isotopic ratios of presolar oxide grains have been reported according to both conventions (e.g., Nittler et al., 1997; Choi et al., 1998). Our present choice was made to make the comparison of the data shown in Figure 2 easier. It furthermore is more natural to use  $^{16}\text{O}$ , which is the primary (and by far most abundant) O isotope, as the reference isotope.

at least 1.2 ppm. Because we found only three presolar corundum grains in the two Murray separates, any abundance estimate for corundum has naturally large uncertainties. Nominally we obtain an abundance of 130 ppb, much larger than the estimates obtained by Nittler (1997) for presolar corundum in various primitive meteorites, which range up to only 30 ppb.

For Murchison KIE we do not have any direct information on the weight fraction relative to the total meteorite. However, we can make a guess based on the abundance of SiC grains in KIE. The EDS spectra indicate that approximately half of the

KIE grains are spinel and about equal numbers of the rest are SiC and  $\text{SiO}_2$ . This is consistent with the identification from the  $(\text{mass-40})^{17}\text{O}^-$  ratios (Fig. 6c) that gives 53% spinel, 27% SiC and 20%  $\text{SiO}_2$ . The absolute abundance of SiC from Murchison in this size range (0.–0.6  $\mu\text{m}$ ) as inferred from the KJ separate series is at most 2 ppm (Amari et al., 1994) and thus KIE cannot be much more than 7 ppm of the whole meteorite. This would imply an abundance of only 30 ppb for presolar spinel and 60 ppb for presolar corundum in KIE. Although it is clear that we are still fighting with the statistics of small numbers and other uncertainties, there is a large discrepancy exceeding all statistical uncertainties both in the abundance of presolar spinel as well as the relative mineralogy of grains between Murray CG and Murchison KIE, two separates with very similar grain sizes from the same type of carbonaceous chondrites. On the CG mount we counted 94 spinel, 4 SiC and 2 corundum grains as identified by EDS. This is consistent with the spinel abundance of 91% in CG based on the  $(\text{mass-40})^{17}\text{O}^-$  ratios. With the 45 ppm abundance of CG as given by Tang and Anders (1988) the resulting total SiC abundance in CG is consistent with the SiC abundance of  $\sim 2$  ppm of this size range in Murchison (Amari et al., 1994). However, the absolute spinel abundance relative to the total meteorite in Murchison KIE is lower by a factor of  $\sim 12$  than in Murray CG and the abundance of presolar spinel grains is correspondingly lower; within statistics, the abundance of presolar spinel as fraction of the analyzed spinel grains is consistent between Murray CG and Murchison KIE (see Table 2). Murchison KIE has undergone much more chemical processing and a possible explanation for this discrepancy would be that spinel grains have been preferentially destroyed relative to SiC. Thus, if most spinel grains of this size range originally present in Murchison were lost during the preparation of the KIE separate, we cannot draw any conclusions about the abundance of presolar spinel in the whole meteorite. The only way to clarify this is to subject Murchison to the same separation procedure to which Murray has been subjected to obtain the residues CF and CG.

In Table 2 we compare the relative and absolute abundances of spinel and corundum grains obtained in this study with those obtained from the analysis of  $\geq 1\text{-}\mu\text{m}$  oxide grains from other meteorites. Sufficiently large numbers of grains were measured only from ordinary chondrites (OCs). For the comparison we used only those data obtained by analysis of all three O isotopes on single grains and excluded those obtained by isotopic imaging of the  $^{18}\text{O}/^{16}\text{O}$  ratio (Nittler, 1996; Nittler et al., 1997). We took all the data from Choi et al. (1998, 1999) and Krestina

Table 2. Fractions of presolar oxide grains.

Meteorite/residue	Spinel/total residue	Corundum/total residue	Spinel/spinel	Spinel/total meteorite	Corundum/total meteorite
Murray CF (0.15 $\mu\text{m}$ )	15/628 (2.4%)	3/628 (0.5%)	15/564 (2.7%)	670 ppb	$\sim 130$ ppb
Murray CG (0.45 $\mu\text{m}$ )	9/753 (1.2%)	0/753 (<0.2%)	9/688 (1.3%)	540 ppb	<90 ppb
Murchison KIE (0.5 $\mu\text{m}$ )	2/473 (0.4%)	4/473 (0.8%)	2/250 (0.8%)	$\sim 30$ ppb	60 ppb
OCs ( $\geq 1 \mu\text{m}$ )			8/1641 (0.5%) <sup>a</sup>	<50 ppb <sup>b</sup>	<6 ppb <sup>b</sup>
Tieschitz ( $\geq 1 \mu\text{m}$ )			1/4000 (<0.1%) <sup>c</sup>		30 ppb <sup>c</sup>

<sup>a</sup> From Krestina et al. (2002) and Krestina and Nittler, unpublished.

<sup>b</sup> From Choi et al. (1), Krestina et al. (2002) and Krestina and Nittler, unpublished; see text.

<sup>c</sup> From Nittler et al. (1997) and Nittler (1997) and Nittler, unpublished.

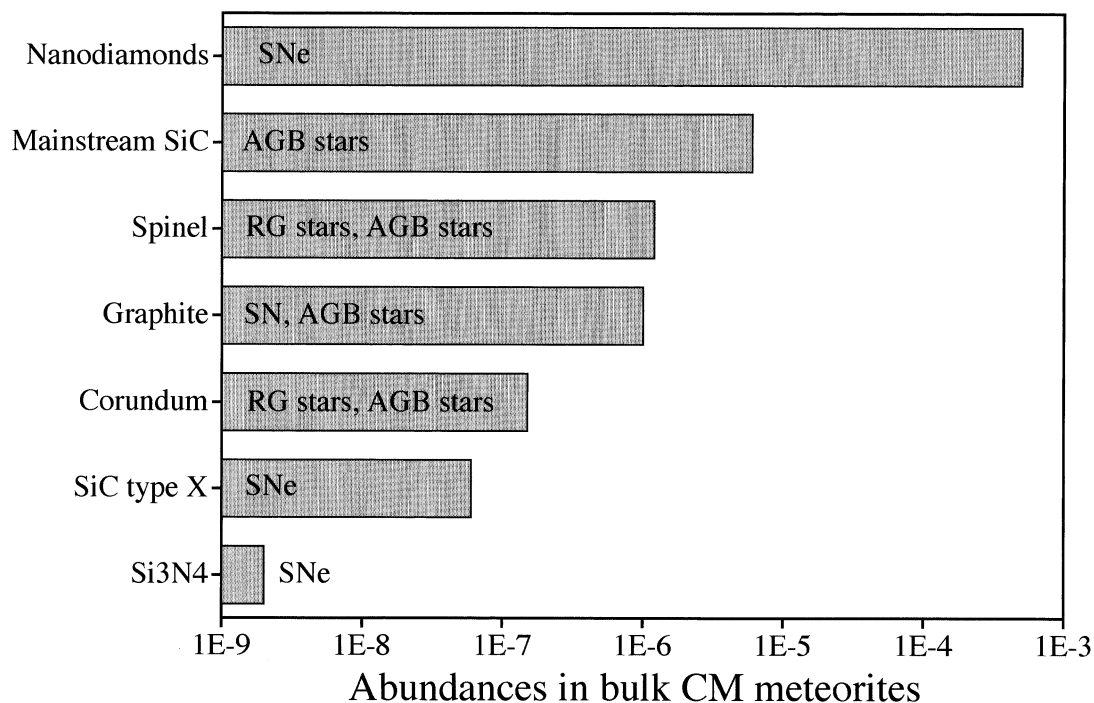


Fig. 8. Abundances of different types of presolar grains in bulk CM carbonaceous chondrites. Our new estimates for the abundances of presolar spinel and corundum have been added to previous estimates for the other grain types (see, e.g., Zinner, 1998). Also indicated are the stellar sources of these grains. Nanodiamonds carry anomalous Xe and Te but, because their bulk C isotopic composition is normal, it is not established whether all nanodiamonds are of stellar origin.

et al. (2002) as well as unpublished data by Krestina and by Nittler obtained on Bishunpur, Krymka, Semarkona, and Tieschitz. These data give 8 presolar spinel grains out of 1641 analyzed and 50 presolar corundum grains out of 2096 analyzed. Unfortunately, any determination of absolute abundances of these presolar grain species as fractions of the whole meteorite is highly uncertain. The reason is that the abundances of spinel and corundum in the analyzed residues are not known. The upper limits given in columns 5 and 6 of Table 2 were obtained by using the relative proportions of spinel, corundum and SiC obtained by Choi et al. (1998) and the abundances of SiC in Semarkona and Bishunpur (Huss, 1997), and by assuming that the fraction of  $\geq 1\text{-}\mu\text{m}$  grains in SiC from these two meteorites is the same as that in SiC in the KJ separate of Murchison (Amari et al., 1994). This last assumption is probably an upper limit. Murchison KJ SiC has a much higher fraction of large grains than SiC from most other meteorites and, although the grain size distribution of SiC from OCs has not been determined,  $^{22}\text{Ne-E}/^{130}\text{Xe-S}$  ratios indicate that SiC from Bishunpur and Semarkona is much finer grained than SiC from the Murchison KJ separate (see Fig. 9 of Russell et al., 1997). The estimates in Table 2 are therefore most likely upper limits and the actual abundances could be as much as an order of magnitude lower.

Based on our new data we can revise the relative abundances of different presolar grain types in CM2 carbonaceous chondrites (e.g., Zinner, 1998), at least based on our results from the Murray separates (Fig. 8). According to these results, presolar spinel appears to be at least as abundant as presolar graphite

and is not as rare as has previously been assumed. There are several reasons for this. One is of course that, as with presolar SiC, presolar spinel seems to consist mostly of submicron grains and only the NanoSIMS has made it possible to locate these. Another possible reason is that the main aim in performing the Murchison K-series and similar separations was to track the carriers of Ne-E and Xe-S, namely presolar SiC and graphite, and the production of spinel separates was of no special concern. The Murray separates might be the best spinel separates presently available.

In Figure 9 we plot the O isotopic ratios of the 26 presolar spinel grains identified in this work together with 11 spinel grains of other studies and compare them to ratios of presolar corundum and hibonite. From the figure it appears that the distribution of the spinel grains is quite different from that of the corundum grains, especially as the relative abundance of grains with low  $^{18}\text{O}/^{16}\text{O}$  ratios is concerned. However, this conclusion is misleading. The reason is that, with the exception of two, all spinel grains were identified in the so-called single grain mode by measuring all three O isotopes. In contrast, only about half the corundum grains were identified in this way, the rest were identified by direct imaging of  $^{16}\text{O}$  and  $^{18}\text{O}$  (Nittler et al., 1997). Because there are many presolar oxide grains with nearly normal  $^{18}\text{O}/^{16}\text{O}$  ratios but large anomalies in the  $^{17}\text{O}/^{16}\text{O}$  ratio, this method tends to miss a substantial fraction of presolar oxide grains and results in a biased distribution of the O isotopic ratios. This is clearly demonstrated in Figure 10, which compares O isotopes of corundum grains identified by these two methods.



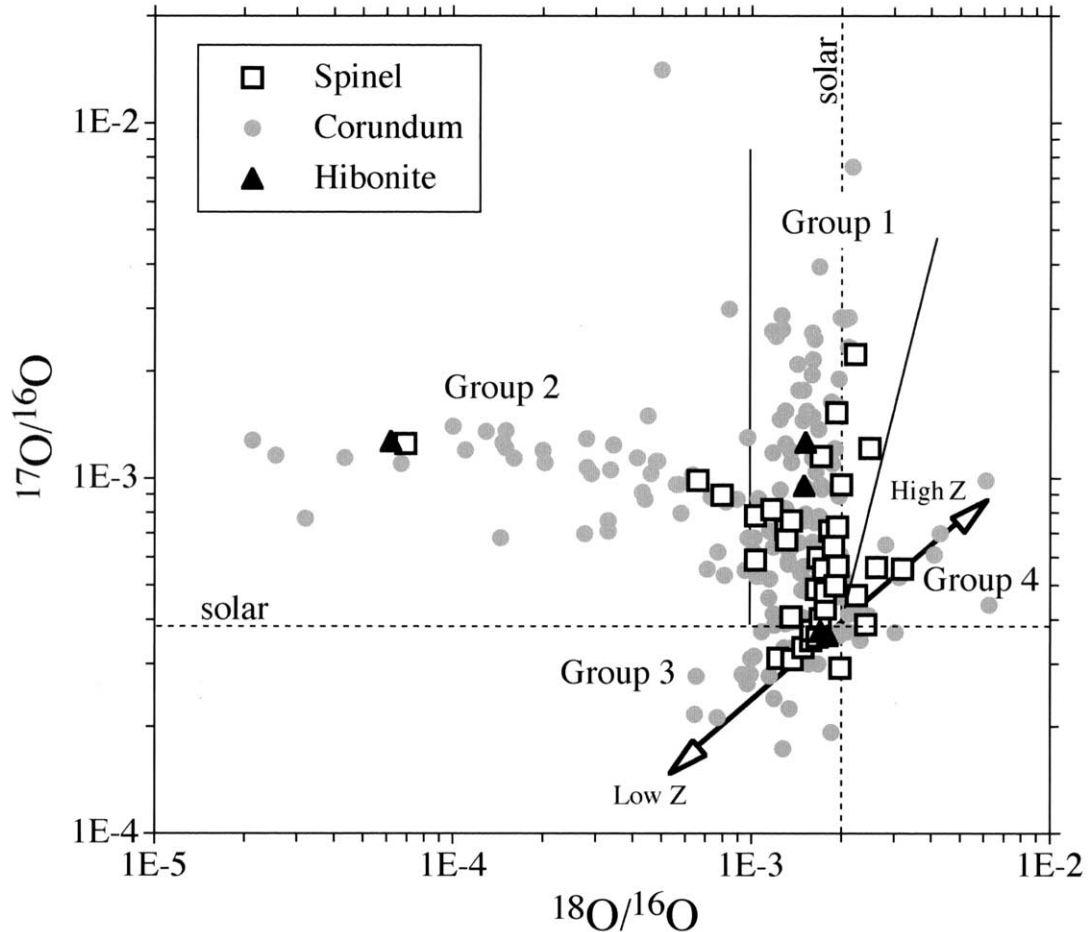


Fig. 9. Comparison of the O isotopic compositions of presolar spinel, corundum, and hibonite. Data are from this study and from Huss et al. (1994), Nittler et al. (1997), and Nittler and Alexander (1999), Choi et al. (1998, 1999), Krestina et al. (2002), and unpublished data by Krestina, Nittler, and Strebel. The four groups defined by Nittler et al. (1997) are indicated. The line with two arrows indicates the galactic evolution of the O isotopes from low metallicity ( $Z$ ) to high metallicity (Timmes et al., 1995). One presolar corundum grain is not shown in this figure; it lies off-scale at  $^{17}\text{O}/^{16}\text{O} = 3.0 \times 10^{-5}$  and  $^{18}\text{O}/^{16}\text{O} = 3.4 \times 10^{-4}$  and has been attributed to a supernova (Nittler et al., 1998).

In Figure 11 we therefore compare spinel ratios only with those of corundum grains that have been identified by single grain measurements. Members of all four groups defined by Nittler (1997) (see Fig. 9) are present. Within the statistical limits imposed by the number of presolar spinel grains identified so far it is difficult to say whether there are any significant differences between spinel and corundum in the distribution of their O isotopic ratios. One difference that is outside statistics concerns grains with large  $^{17}\text{O}/^{16}\text{O}$  ratios: among the corundum grains in Figure 11, 18 out of 89 (20%) have  $^{17}\text{O}/^{16}\text{O}$  ratios  $> 1.5 \times 10^{-3}$  but only 2 out of 37 (5%) among the spinel grains. This indicates that a larger fraction of corundum grains comes from stars with larger mass ( $1.8 M_{\odot} < M < 4.5 M_{\odot}$ ) than spinel grains because the first dredge-up in stars within this mass range results in higher  $^{17}\text{O}/^{16}\text{O}$  ratios (Boothroyd et al., 1994; Boothroyd and Sackmann, 1999). According to the models by these authors,  $^{17}\text{O}/^{16}\text{O}$  ratios increase again for higher masses but it is unlikely that grains with  $^{17}\text{O}/^{16}\text{O} < 1.5 \times 10^{-3}$  come from stars with  $M > 4.5 M_{\odot}$ .

Only one spinel grain has the large  $^{18}\text{O}$  depletion exhibited

by corundum grains, especially those identified by ion imaging (Fig. 10). But the relative abundances of group 2 grains (defined as having  $^{18}\text{O}/^{16}\text{O}$  ratios  $< 10^{-3}$  and  $^{17}\text{O}/^{16}\text{O}$  ratios higher than solar), whose O ratios may be explained by cool bottom processing (Wasserburg et al., 1995; Nollett et al., 2003) and/or hot bottom burning (Boothroyd and Sackmann, 1999), are comparable, 3 of 37 (8%) for spinel and 8 of 89 (9%) for corundum. Spinel grains do not extend to  $^{16}\text{O}$ -rich compositions (group 3) to the degree corundum grains do although the relative abundances of group 3 grains are comparable among these two grain types. We note that the two corundum grains with the largest  $^{16}\text{O}$  enrichments in Figure 11 (black circles) are from the Murray CF residue (see Fig. 5a). However, corundum group 3 grains with even lower  $^{17}\text{O}/^{16}\text{O}$  ratios are found among grains identified by ion imaging. Group 3 grains have been interpreted as originating from low-metallicity stars (Nittler et al., 1997) and one corundum grain with large  $^{16}\text{O}$  excesses has been attributed to a supernova (Nittler et al., 1998). Because the  $^{17}\text{O}/^{16}\text{O}$  and  $^{18}\text{O}/^{16}\text{O}$  ratios increase as the Galaxy evolves (Timmes et al., 1995), this implies that essentially all group 3

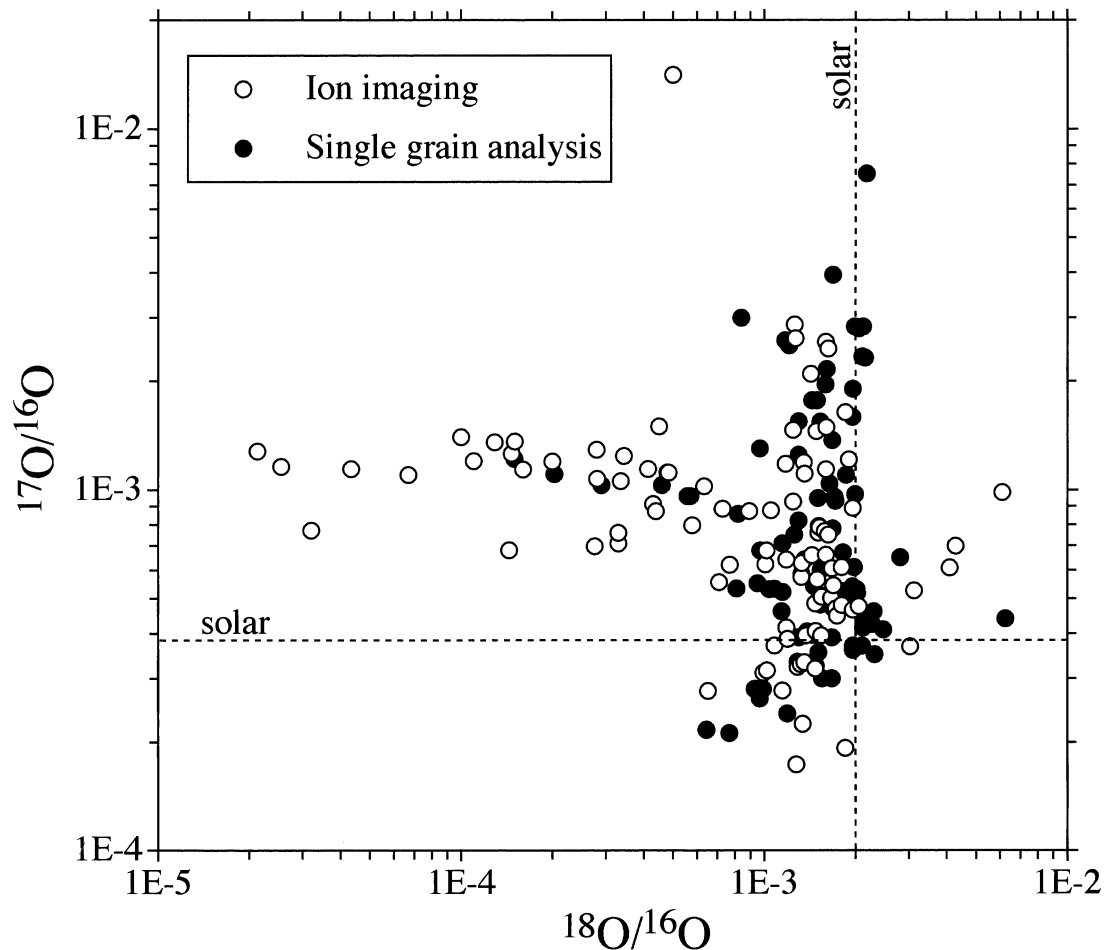


Fig. 10. Comparison of the O isotopic ratios of presolar corundum grains that were identified by ion imaging of  $^{16}\text{O}$  and  $^{18}\text{O}$  and those that were identified by single grain measurement of all three O isotopes. In the ion imaging method, grains with close to normal  $^{18}\text{O}/^{16}\text{O}$  ratios but anomalous  $^{17}\text{O}/^{16}\text{O}$  ratios are missed.

grains come from older (and therefore lower-mass) stars than grains in the other groups. Conversely, group 4 grains, grains with  $^{17}\text{O}$  and  $^{18}\text{O}$  excesses, could come from stars with higher-than-solar metallicity but it is unlikely for stars older than the sun to have the high metallicity required by the compositions of some grains (see Fig. 9). Depending on how one extrapolates the dependence of the O isotopic ratios on metallicity (see Fig. 12 of Timmes et al., 1995), O isotopic ratios a factor of 2 to 3 higher than solar imply metallicities up to  $Z = 0.06$ , significantly higher than what is expected for stars older than our sun in the solar neighborhood (Edvardsson et al., 1993). Alternatively, they could either come from low-mass stars, in which  $^{18}\text{O}$  produced by He burning of  $^{14}\text{N}$  during early pulses was mixed into the envelope by third dredge-up (Boothroyd and Sackmann, 1988) or, more likely, have a supernova origin as suggested by Choi et al. (1998). The group 4 spinel grains have smaller  $^{17}\text{O}$  and  $^{18}\text{O}$  excesses than some corundum grains. Without any additional isotopic features a specific stellar origin cannot be determined for them. Overall, there does not appear to be a drastic difference in the O isotopic ratio distribution of spinel and corundum grains.

## 5. FUTURE PERSPECTIVES

Although this study has significantly increased the number of presolar spinel grains, it would be highly desirable to identify larger numbers of such grains. One reason is to obtain better statistics on the distribution of their O isotopic compositions to determine whether or not there are systematic differences between presolar spinel and corundum. Another goal is to better determine the abundance of presolar spinel and corundum as a function of grain size. We plan to measure also grains from the next-largest Murray grain size fraction, CH (Tang and Anders, 1988; see Fig. 1). In addition, we will try to obtain a better identification of the grains' mineralogy. We will be able to measure also the  $\text{AlO}^-$  signal along with the  $\text{O}^-$  and  $\text{MgO}^-$  signals. As already mentioned, we will also try positive secondary ion imaging of Mg, Al, Si, and Ca on the same grains.

The amassing of isotopic data on large numbers of grains will require implementation of automatic imaging searches. This will be especially important if we want to detect a reasonable number of small presolar corundum grains (in CG they appear to be only 1–2% of spinel). Automatic isotopic imaging in a raster mode by single grain measurements has been dem-

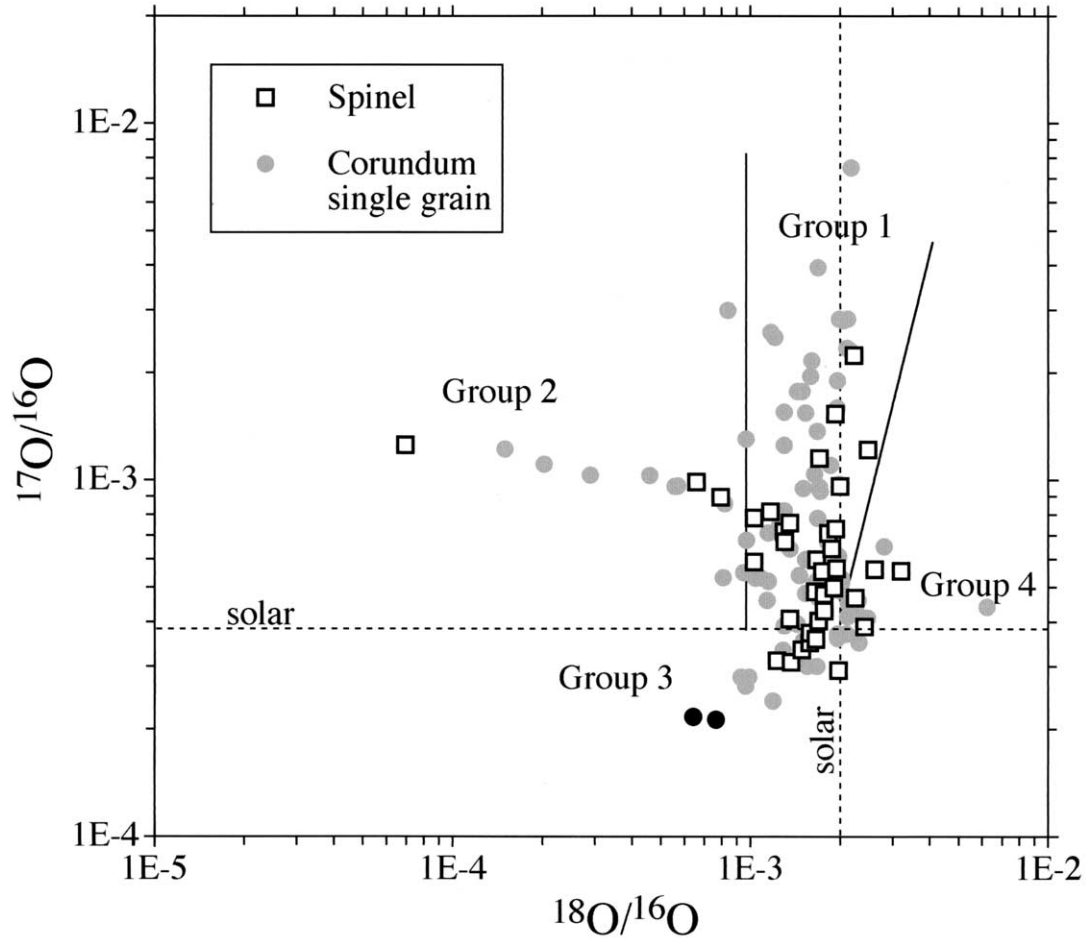


Fig. 11. Comparison of the O isotopic ratios of presolar spinel grains with those of presolar corundum grains identified by single grain analysis of all three O isotopes. Data are from Huss et al. (1994), Nittler et al. (1997), and Nittler and Alexander (1999), Choi et al. (1998, 1999), Krestina et al. (2002), and unpublished data by Krestina, Nittler, and Strelbel. Except for grains with  $^{17}\text{O}/^{16}\text{O} > 2 \times 10^{-3}$  the distributions are very similar. The two black circles on the lower left are corundum grains from Murray CF.

onstrated on a Cameca ims 6f ion microprobe (Nittler and Alexander, 1999). However, it will require major software development for the NanoSIMS. As far as the analysis of small corundum grains is concerned, it certainly would help if they could be concentrated by separating them from spinel. The densities of these two minerals are different ( $3.97 \text{ g/cm}^3$  for corundum and  $3.6 \text{ g/cm}^3$  for spinel) but probably too close to achieve separation for submicron grains. Only larger ( $> 2 \mu\text{m}$ ) corundum grains seem to survive the treatment with sulfuric acid that was used to destroy spinel and obtain the KJ SiC fractions (Amari et al., 1994). Corundum grains  $< 1 \mu\text{m}$  in size were apparently destroyed along with spinel. Different acid treatments must be tested to see whether spinel can be preferentially dissolved.

We now have evidence for the presence of presolar corundum, hibonite, and spinel in primitive meteorites. These, together with melilite, are the minerals that are expected to condense first during the cooling of a gas of solar composition (Grossman, 1972; see also Wood and Hashimoto, 1993). The same condensation sequence must hold for the atmospheres of O-rich red giant and AGB stars. Presolar melilite has not been

identified in primitive meteorites nor have other presolar silicates although astronomical observations indicate the presence of crystalline forsterite and enstatite in circumstellar dust shells of evolved stars (e.g., Molster, 2000; Kemper et al., 2001). However, presolar silicates, among them a forsterite grain, have recently been found in interplanetary dust particles (Messenger et al., 2003). There are several possible reasons for the fact that presolar silicates have not been identified in meteorites. One is that silicates, which are more likely to be affected by alteration processes in the solar system and on parent bodies than the refractory phases identified as presolar grains, simply did not survive. Even if this is not the case, they could easily have been missed. Previous searches for presolar silicates were mostly made on grains  $> 1 \mu\text{m}$  (Nittler, 1996; Messenger and Bernatowicz, 2000). However, the present work shows that the abundances of presolar spinel (and probably corundum) increase with decreasing grain size and the same has previously been shown for presolar SiC (Amari et al., 1994). Nevertheless, even if presolar silicates in meteorites were as large as  $1 \mu\text{m}$  they still would not have been detected if their abundance were as low as that of presolar spinel ( $\sim 1 \text{ ppm}$ ). Thorough isotopic

searches of submicron silicate grains, preferentially enriched in the most likely candidate minerals melilite, forsterite and enstatite, might yet lead to the identification of presolar silicates in meteorites.

## 6. CONCLUSIONS

By measuring the O isotopic compositions of submicron grains in acid residues from the carbonaceous chondrites Murray and Murchison in the NanoSIMS we identified 26 presolar spinel grains, increasing the number of known presolar spinel to 37. The abundance of presolar spinel as a fraction of all spinel grains increases with decreasing grain size. The abundance of presolar spinel in Murray is  $>1.2$  ppm of the total meteorite, at least as high as that of presolar graphite, and much higher than had previously been believed. The O-isotopic distribution of the spinel grains is very similar to those of presolar corundum; the only statistically significant difference appears to be that there is a larger fraction of corundum grains with large  $^{17}\text{O}$  excesses ( $^{17}\text{O}/^{16}\text{O} > 1.5 \times 10^{-3}$ ), which indicates parent stars with masses between 1.8 and 4.5  $M_{\odot}$ .

*Acknowledgments*—This work constitutes one of the first scientific applications of a new type of ion microprobe, the NanoSIMS, which was recently installed in our laboratory. It would not have been possible without the original design of the instrument by Georges Slodzian of the University of Paris at Orsay and the efforts of François Hillion of Cameca, Paris to accommodate our requirements. For funding for the acquisition of the NanoSIMS we are grateful to the McDonnell Center for the Space Sciences, NASA and NSF. We thank Tang Ming for producing the Murray CF and CG residues and Natasha Krestina, Larry Nittler, and Roger Strelbel for providing unpublished data on presolar oxide grains. Reviews by Peter Hoppe, Larry Nittler, Uli Ott and an anonymous reviewer have helped in improving the manuscript and are gratefully acknowledged. This work was supported by NASA grant NAG5-11545.

*Associate editor:* U. Ott.

## REFERENCES

- Amari S., Lewis R. S., and Anders E. (1994) Interstellar grains in meteorites: I. Isolation of SiC, graphite, and diamond; size distributions of SiC and graphite. *Geochim. Cosmochim. Acta* **58**, 459–470.
- Baertschi P. (1976) Absolute  $^{18}\text{O}$  content of standard mean ocean water. *Earth Planet. Sci. Lett.* **31**, 341–344.
- Bernatowicz T., Fraundorf G., Tang M., Anders E., Wopenka B., Zinner E., and Fraundorf P. (1987) Evidence for interstellar SiC in the Murray carbonaceous meteorite. *Nature* **330**, 728–730.
- Boothroyd A. I. and Sackmann I.-J. (1988) Low-mass stars. III. Low-mass stars with steady mass loss: Up to the asymptotic giant branch and through the final thermal pulses. *Astrophys. J.* **328**, 653–670.
- Boothroyd A. I. and Sackmann I.-J. (1999) The CNO isotopes: Deep circulation in red giants and first and second dredge-up. *Astrophys. J.* **510**, 232–250.
- Boothroyd A. I., Sackmann I.-J., and Wasserburg G. J. (1994) Predictions of oxygen isotope ratios in stars and of oxygen-rich interstellar grains in meteorites. *Astrophys. J.* **430**, L77–L80.
- Choi B.-G., Huss G. R., Wasserburg G. J., and Gallino R. (1998) Presolar corundum and spinel in ordinary chondrites: Origins from AGB stars and a supernova. *Science* **282**, 1284–1289.
- Choi B.-G., Wasserburg G. J., and Huss G. R. (1999) Circumstellar hibonite and corundum and nucleosynthesis in asymptotic giant branch stars. *Astrophys. J.* **522**, L133–L136.
- Clayton R. N. and Mayeda T. K. (1984) The oxygen isotope record in Murchison and other carbonaceous chondrites. *Earth Planet. Sci. Lett.* **67**, 151–161.
- Edvardsson B., Anderson J., Gustafsson B., Lambert D. L., Nissen P. E., and Tomkin J. (1993) The chemical evolution of the galactic disk. I. Analysis and results. *Astron. Astrophys.* **275**, 101–152.
- Grossman L. (1972) Condensation in the primitive solar nebula. *Geochim. Cosmochim. Acta* **36**, 597–619.
- Huss G. R. (1997) The survival of presolar grains in solar system bodies. In *Astrophysical Implications of the Laboratory Study of Presolar Materials* (eds. T. J. Bernatowicz and E. Zinner), pp. 721–748. AIP, New York.
- Huss G. R., Fahey A. J., Gallino R., and Wasserburg G. J. (1994) Oxygen isotopes in circumstellar  $\text{Al}_2\text{O}_3$  grains from meteorites and stellar nucleosynthesis. *Astrophys. J.* **430**, L81–L84.
- Hutcheon I. D., Huss G. R., Fahey A. J., and Wasserburg G. J. (1994) Extreme  $^{26}\text{Mg}$  and  $^{17}\text{O}$  enrichments in an Orgueil corundum: Identification of a presolar oxide grain. *Astrophys. J.* **425**, L97–L100.
- Kemper F., Waters L. B. F. M., de Koter A., and Tielens A. G. G. M. (2001) Crystallinity versus mass-loss rate in Asymptotic Giant Branch stars. *Astron. Astrophys.* **369**, 132–141.
- Krestina N., Hsu W., and Wasserburg G. J. (2002) Circumstellar oxide grains in ordinary chondrites and their origin. *Lunar Planet. Sci.* **33**, abstract #1425.
- Messenger S. and Bernatowicz T. J. (2000) Search for presolar silicates in Acfer 094. *Meteorit. Planet. Sci.* **35**, A109.
- Messenger S., Keller L. P., Stadermann F. J., Walker R. M., and Zinner E. (2003) Samples of stars beyond the solar system: Silicate grains in interplanetary dust. *Science* **300**, 105–108.
- Molster F. J. (2000) Crystalline silicates. New probes of circumstellar dust conditions?. In *ISO Beyond the Peaks* (eds. A. Salama, M. F. Kessler, K. Leech, and B. Schulz), pp. 151–154. Villafranca del Castillo, Spain.
- Nittler L. R. (1996) *Quantitative Isotopic Ratio Ion Imaging and Its Application to Studies of Preserved Stardust in Meteorites*. Ph.D. thesis, Washington University.
- Nittler L. R. (1997) Presolar oxide grains in meteorites. In *Astrophysical Implications of the Laboratory Study of Presolar Materials* (eds. T. J. Bernatowicz and E. Zinner), pp. 59–82. AIP, New York.
- Nittler L. R. and Alexander C. M. O'D. (1999) Automatic identification of presolar Al- and Ti-rich oxide grains from ordinary chondrites. *Lunar Planet. Sci.* **30**, abstract #2041.
- Nittler L. R., Alexander C. M. O'D., Gao X., Walker R. M., and Zinner E. K. (1994) Interstellar oxide grains from the Tieschitz ordinary chondrite. *Nature* **370**, 443–446.
- Nittler L. R., Alexander C. M. O'D., Gao X., Walker R. M., and Zinner E. (1997) Stellar sapphires: The properties and origins of presolar  $\text{Al}_2\text{O}_3$  in meteorites. *Astrophys. J.* **483**, 475–495.
- Nittler L. R., Alexander C. M. O'D., Wang J., and Gao X. (1998) Meteoritic oxide grain from supernova found. *Nature* **393**, 222.
- Nollett K. M., Busso M., and Wasserburg G. J. (2003) Cool bottom processes on the thermally pulsing asymptotic giant branch and the isotopic composition of circumstellar dust grains. *Astrophys. J.* **582**, 1036–1058.
- Russell S. S., Ott U., Alexander C. M. O'D., Zinner E. K., Arden J. W., and Pillinger C. T. (1997) Presolar silicon carbide from the Indarch (EH4) meteorite: Comparison with silicon carbide populations from other meteorite classes. *Meteorit. Planet. Sci.* **32**, 719–732.
- Slodzian G., Hillion F., Stadermann F. J., and Horreard F. (2003) Oxygen isotopic measurements on the CAMECA Nanosims 50. *Appl. Surf. Sci.* **203–204**, 798–801.
- Stadermann F. J., Walker R. M., and Zinner E. (1999a) NANOSIMS: The next generation ion probe for the microanalysis of extraterrestrial material. *Meteorit. Planet. Sci.* **34**, A111–A112.
- Stadermann F. J., Walker R. M., and Zinner E. (1999b) Sub-micron isotopic measurements with the CAMECA NanoSIMS. *Lunar Planet. Sci.* **30**, abstract #1407.
- Stadermann F. J., Walker R. M., and Zinner E. (2000) NANOSIMS: A new generation ion probe for the microanalysis of natural materials. *Beyond 2000—New Frontiers in Isotope Geoscience*.
- Tang M. and Anders E. (1988) Isotopic anomalies of Ne, Xe, and C in meteorites. II. Interstellar diamond and SiC: Carriers of exotic noble gases. *Geochim. Cosmochim. Acta* **52**, 1235–1244.
- Tang M., Lewis R. S., Anders E., Grady M. M., Wright I. P., and Pillinger C. T. (1988) Isotopic anomalies of Ne, Xe, and C in meteorites. I. Separation of carriers by density and chemical resistance. *Geochim. Cosmochim. Acta* **52**, 1221–1234.

- Timmes F. X., Woosley S. E., and Weaver T. A. (1995) Galactic chemical evolution: Hydrogen through zinc. *Astrophys. J.* **98**, (Suppl.), 617–658.
- Wasserburg G. J., Boothroyd A. I., and Sackmann I.-J. (1995) Deep circulation in red giant stars: A solution to the carbon and oxygen isotope puzzles? *Astrophys. J.* **447**, L37–L40.
- Wood J. A. and Hashimoto A. (1993) Mineral equilibrium in fractionated nebular systems. *Geochim. Cosmochim. Acta* **57**, 2377–2388.
- Zinner E. (1998) Stellar nucleosynthesis and the isotopic composition of presolar grains from primitive meteorites. *Ann. Rev. Earth Planet. Sci.* **26**, 147–188.
- Zinner E. and Tang M. (1988) Anomalous oxygen in spinels from a Murray separate. *Lunar Planet. Sci.* **29**, 1323–1324.
- Zinner E., Tang M., and Anders E. (1987) Large isotopic anomalies of Si, C, N and noble gases in interstellar silicon carbide from the Murray meteorite. *Nature* **330**, 730–732.